Reeling-induced residual stress and its effect on the fracture behavior of pipes with through thickness cracks

Z. L. Zhang[1], E. Østby[2], B. Nyhus[2], J. Ødegård[2] and R. Verley[3]
[1]Faculty of Engineering Science and Technology, Norwegian University of Science (NTNU), [2]SINTEF Materials Technology, and [3]Statoil Research Center, Trondheim, Norway
E-mail: zhiliang.zhang@ntnu.no

Abstract – Treatment of residual stresses in the failure assessment of pipelines is a complex issue: neglecting residual stress may become non-conservative while assessment based on the measured peak residual stress value often results in an over estimation. In this paper, the residual stress field due to a typical pipe reeling process and its effect on the fracture behavior of pipes with through thickness cracks have been studied by three-dimensional finite element analyses. Various parameters that affect the peak residual stress value and residual stress distribution have been studied first. A representative residual stress field was then applied to study the effect on the fracture behavior of pipes with through thickness cracks. The residual stress field has been rotated with respect to the crack tip location to identify the most critical position. Contact elements were used to simulate the partial contact of crack surfaces caused by the compressive residual stresses. It has been shown that neglecting the contacts between the crack surfaces will not cause a significant error when external load is applied. The critical crack tip driving force caused by the residual stress field is very small compared with the failure assessment result based on the peak residual stress.

1. Introduction

Treatment of residual stress is an important and yet difficult subject in failure assessment of pipelines. It is difficult to measure correctly [1]. Residual stress is a self-balanced stress field, and has a complicated distribution and strong gradient. It is often characterized by its peak values, which then are used in failure assessment. The peak residual stress is commonly assumed to be equal to the value of yield stress of the material. In many cases, assessment using the peak value may yield over-conservative estimation.

A relatively simple case where the residual stress is caused by a reeling process is considered in this paper. Reeling is an industrial process where pipe is reeled to a large wheel and then straightened to the ground [2]. Reverse plastic deformation cycles resulted in the final residual stress field. The residual stresses in a pipe due to a reeling process and their effect on the fracture behavior of a pipe section containing a through thickness crack have been studied. Three dimensional finite element analyses were used to simulate the reeling-induced residual stress field and various parameters which influence the peaks stresses and residual stress distribution have been investigated. A typical distribution pattern of the residual stress field caused by the reeling process was then applied to study the effect on fracture behavior of a pipe section with through thickness cracks. Three relatively large through thickness crack sizes have been analyzed.

2. Simulation of the reeling process

The simulations were carried out using a three-dimensional finite element model of a pipe section without crack, Fig. 1. We consider a 9" steel pipe with a wall thickness 15.6 mm and inside diameter / wall thickness ratio 14.7. The length of the pipe section simulated is four times the pipe diameter. Due to the symmetry only half of the pipe segment is modeled. 8 node brick elements in ABAQUS were used in the analyses. Non-linear geometrical effects were included in the simulation. To simulate the reeling process the model was loaded in pure bending. This was obtained by prescribing a Multi Point Constraint (MPC) at one end of the pipe segment. This MPC forces all the nodes at this end to remain in the same plane during deformation, however, the pipe is free to deform in this plane. The bending was introduced by prescribing a rotation to a node in the centre of the pipe segment, which was transferred to the pipe through the MPC connection described above. The E-modulus was assumed to be 200000 MPa, and the Poisson ration 0.3. An isotropic plasticity model with power law hardening was assumed in most of the analyses.

A typical industrial reeling process contains several loading and unloading cycles. Table 1 presents the representative cycles used in the parameter study. A positive *R* value gives tensile strains at 12 o'clock position of the pipe, while a negative *R* gives compressive strains in the same position.

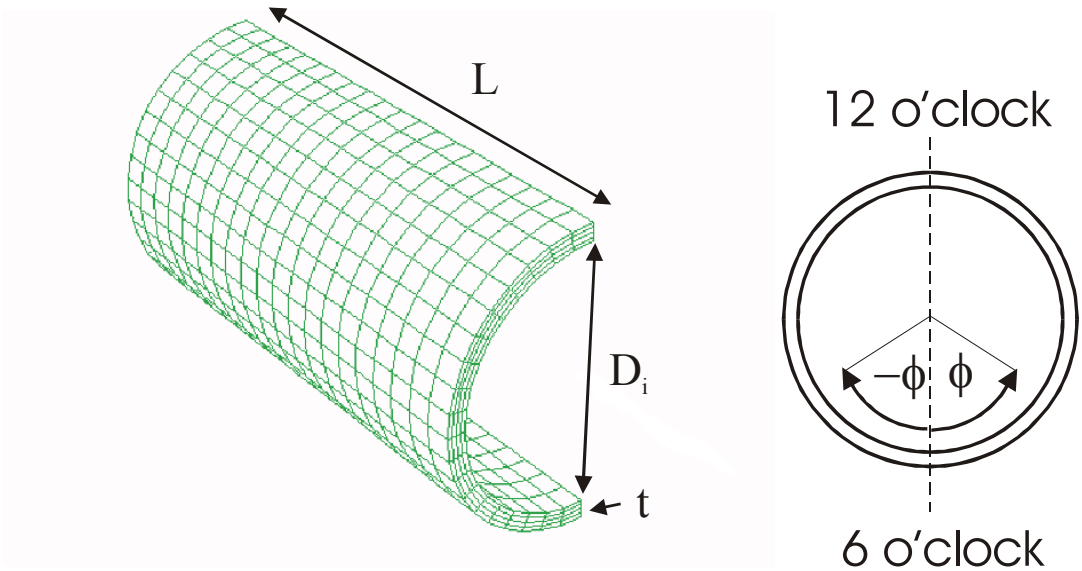

Figure 1 a) The FE model applied to simulate residual stresses due to the reeling process, b) pipe cross section position definition.

Table 1 A representative reeling cycle

Steps	Reeling curvature radius *R* / pipe outer radius *r*	Maximum pipe axial strain at 12 o'clock position
A	-200	-0.005
B	60	0.017
C	∞	0
D	50	0.020
E	-200	-0.005
F	∞	0

Fig. 2 shows the typical axial stress versus axial strain curves at 12 o'clock position resulted from a material with yield stress 600 MPa and hardening exponent 0.1. It can be seen that significant hardening has been experienced for this material at step D with a maximum axial stress over 1.3 times the yield stress. Fig. 3 compares the axial residual stress distributions of the same material at different locations. It can be seen that between 8 and 10 o'clock the axial residual stresses are homogenous through the thickness. There is a relatively large variation through the thickness at 6 and 12 o'clock. The peak tensile stresses appeared at approximately 8 o'clock and 12 o'clock. The negative stress peaks occurs at 6 and approximately 10 o'clock. The difference between the maximum tensile peak stress and the compressive peak is about 1.3 times the yield stress. In the following, the residual stress distribution at the middle section will be focused.

The effect of strain hardening on the final residual stress distribution has also been studied, Fig. 4. Both isotropic and kinematic hardening models have been used. It is interesting to observe that the peak residual stress values at 8 and 10 o'clock are not significantly influenced by the hardening models. However, the residual stress values at 6 and 12 o'clock will be reduced when materials strain hardening is increased. In contradiction, kinematic hardening model will increase the residual stress values at 6 and 12 o'clock.

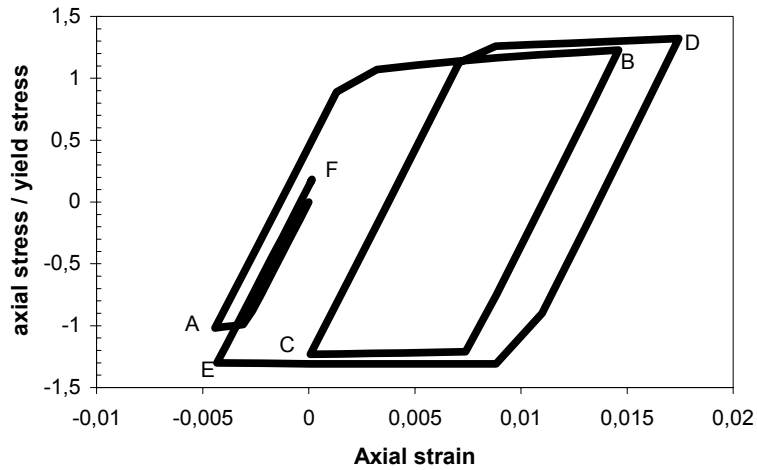

Figure 2 Typical reeling cycles for the axial-stress strain curve at the 12 o'clock position.

The yield stress has an important effect on the final residual stress distribution, Fig. 5. Under the given reeling cycle (Table 1), Fig. 5 shows that the residual stress distribution along the cross section will become smoother for the case with materials with higher yield strength. This observation is also in agreement with Fig. 4, where material with high strain hardening will yield lower residual stresses at 6 and 12 o'clock. This observation can be explained by the fact that the stronger the material the more elastically the material behaves.

In general, it can be observed that the peak yield stresses at 8 and 10 o'clock positions are about between 50 and 60% of the yield stress. For very low yield strength materials with low strain hardening, the peak residual stresses at 6 and 12 o'clock positions can approach the value 1.2 times of the initial yield strength.

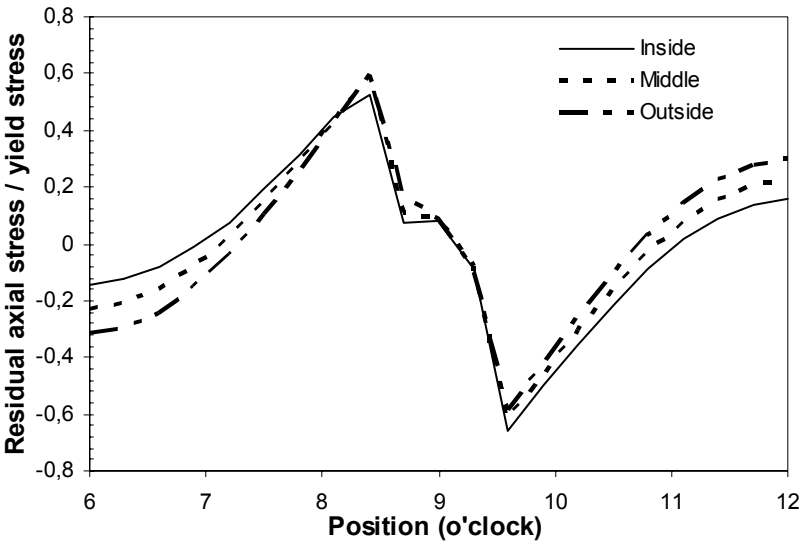

Figure 3 Distribution of the residual stress at different thickness positions.

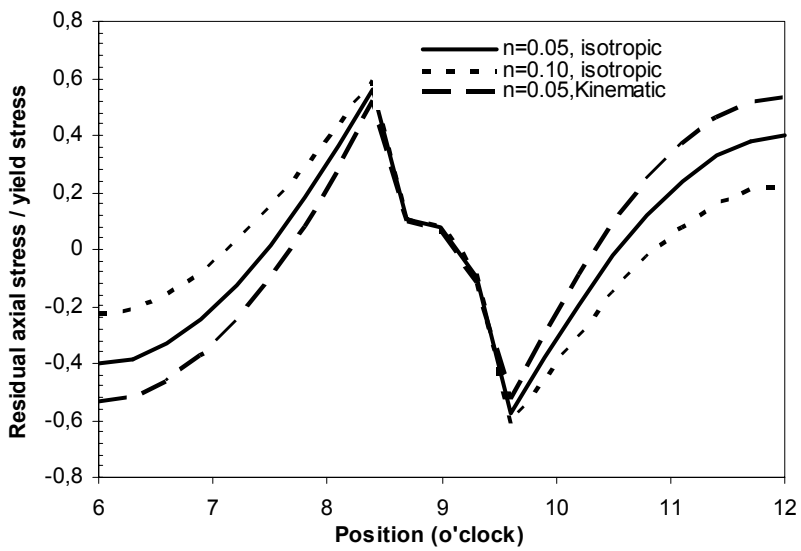

Figure 4 Effect of hardening on the final residual stress distribution.

In the following, in order to illustrate the residual stress effect, the residual stress distribution pattern of the material with yield strength 400 MPa and hardening n=0.05 has been used for studying the effect of residual stress on the fracture behavior of pipe sections with through thickness cracks.

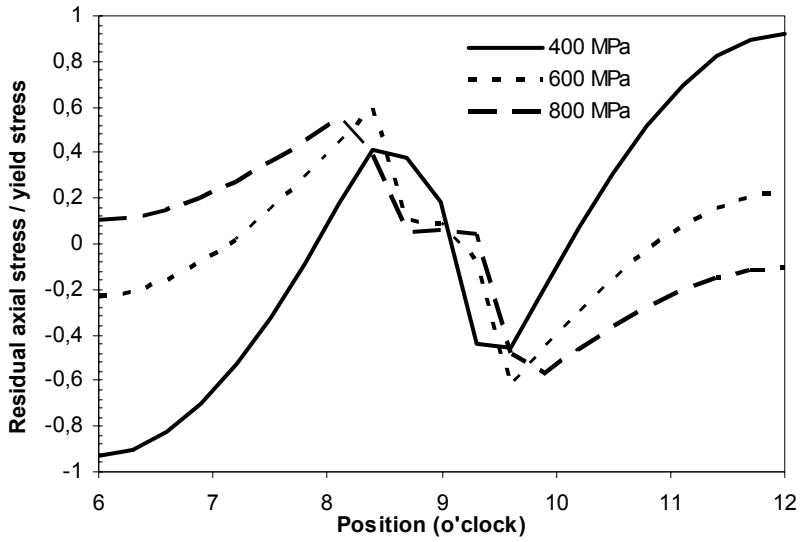

a)

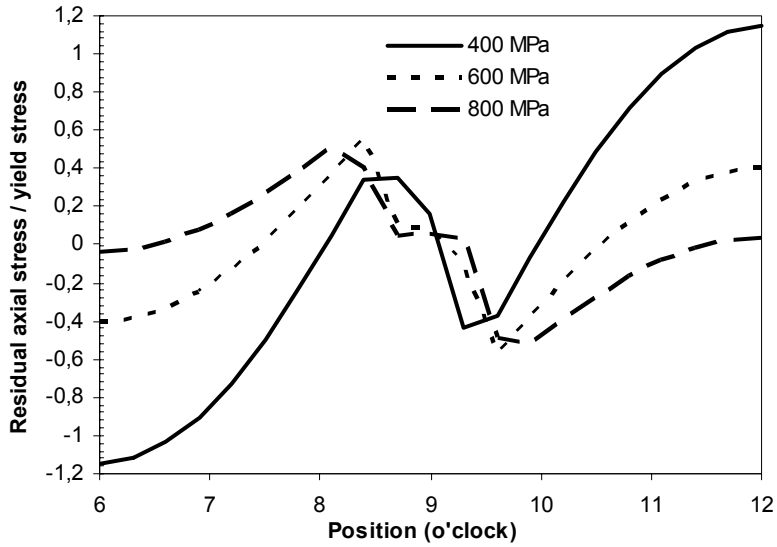

b)

Figure 5 Effect of yield stress on the residual stress distribution a) hardening n=0.1, b) n=0.05.

3. Effect of residual stresses on fracture behavior

In failure assessment, a uniform axial residual stress characterized by the peak stress value is used for calculating the crack tip driving force. In the following, the crack tip driving force caused by the real residual stress field will be calculated and compared with the failure assessment results. The residual stress along the pipe thickness was assumed to be constant. In order to consider the asymmetric condition of the residual

stress with respect to the crack tip, full pipe cross section was modeled. Two steps were used in the ABAQUS analyses. In the first step, the crack was closed and the residual stress field was inputted to the ABAQUS as an initial stress field. In this case, ABAQUS performs analyses to adjust the initial stress field and reach a self-equilibrium state. The final residual stress state was carefully checked. The crack was opened gradually in the second step. A similar method has been applied by Finch and Burdekin [3,4] for studying the effect of residual stress in a plate panel and tubular joints.

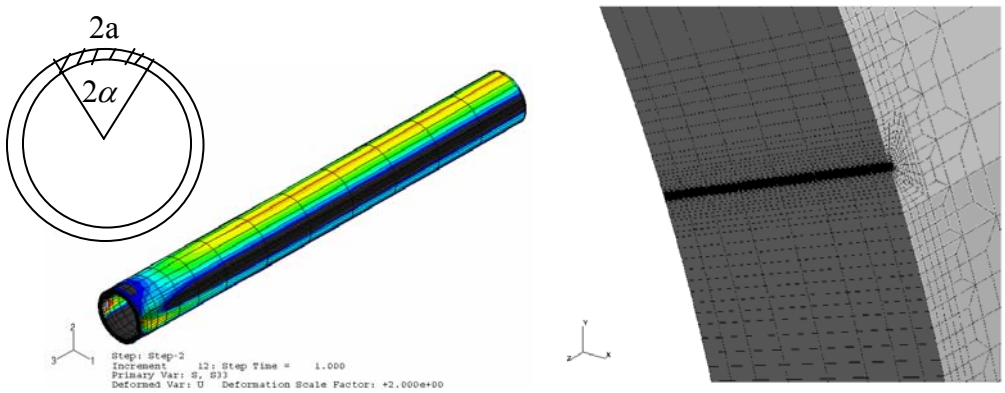

a) b)

Figure 6 3D mesh (½) used in fracture assessment of pipes a) global mesh, b) local mesh arrangement.

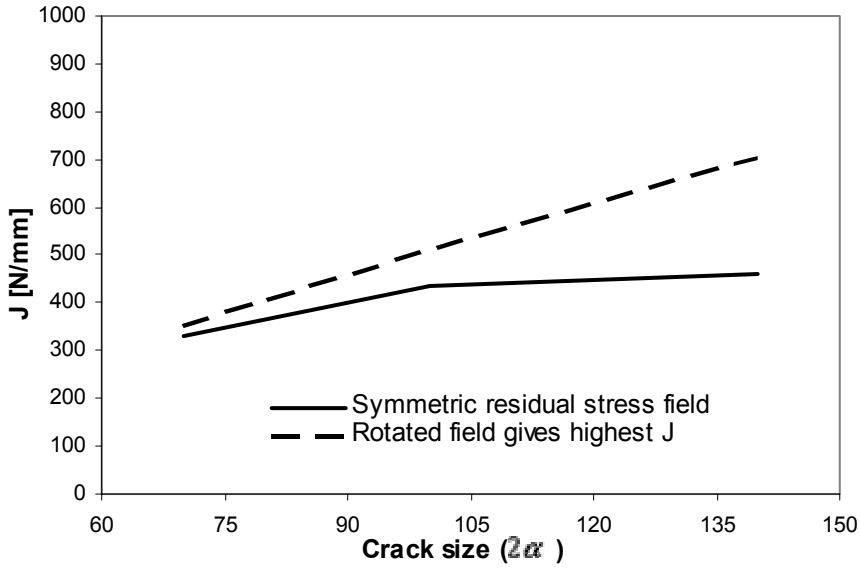

Figure 7 The J values from a symmetrical residual stress field and the highest J value obtained by rotating the residual stress field with respect to the crack tip.

Fig. 6 shows the global mesh (½) and local mesh of the crack models. Three crack sizes have been considered, $2\alpha = 70^\circ$, 100° and 140°. The length of the pipe model was four times the pipe radius. Due to the symmetry only half of the pipe segment is modeled. The remote end of the pipe model was fixed during the residual stress analysis. The crcak tip mesh arrangements for the three crack models are exactly the same. The crack tip was modelled with an initial opening 0.02 mm. The initial yield strength of the material was taken as 400 MPa and the peak residual stress was assumed to be equal to the yield stress unless otherwise specified.

The symmetrical residual stress field has been applied first. For the smallest and medium cracks ($2\alpha = 70^\circ$, 100°) the crack surfaces and crack tips are initaiily situated in the tensile residual field. For the largest crack model, the whole crack face is also initially located in the tensile residual stress field. However, its crack front is close to the compressive residual stress peak. Nevertheless, after a re-distribution of the residual stress field once the crack is introduced, positive J values were obtained for all the three crack models. The resulting J values are plotted in Fig. 7. The J values induced by the symmetrical residual stress field are slightly less influenced by the crack size than the highest J.

In order to study whether asymmetric residual stress fields with respect to the crack tip position will result in dramatic change of the crack tip driving forces, the symmetric residual stress field has been rotated clockwise with respect to the crack.

Fig. 8 shows the effect of the residual stress field position with respect to the crack fronts on the J-integral for the model with the largest crack ($2\alpha = 140^\circ$). It can be seen that the position with a rotated angle 30° resulted in the highest J for this carck model. Similar calculations have been carried out for the other two crack models, and it has been shown that a rotation angle 15° gives the highest J for both the medium and smallest crack models.

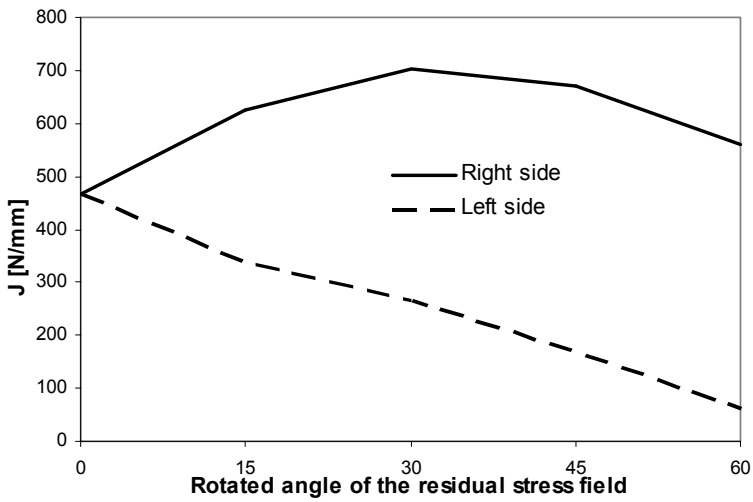

Figure 8 The maximum J at the two crack fronts as a function of the rotated angle of the residual stress field for the crack model with $2\alpha = 140^\circ$.

For each residual stress field position, the maximum J appeared at different locations along the pipe thickness, Fig. 9, where "-1" indicates inside and "1" the outside. It is interesting to note that the highest J does not seem to occur at the middle section. It should be noted that the thickness variation of the residual stress has been neglected in this study. The thickness variation may influence the location where the highest J appears in the thickness.

The highest J values caused by residual stress field for three crack models are compared with the J from the symmetrical residual stress field in Fig. 7. When the crack size is small, the J from the symmetrical residual stress field is very close to the highest J. For the largest crack model, the J from the symmetrical residual stress field is only 2/3 of the highest J.

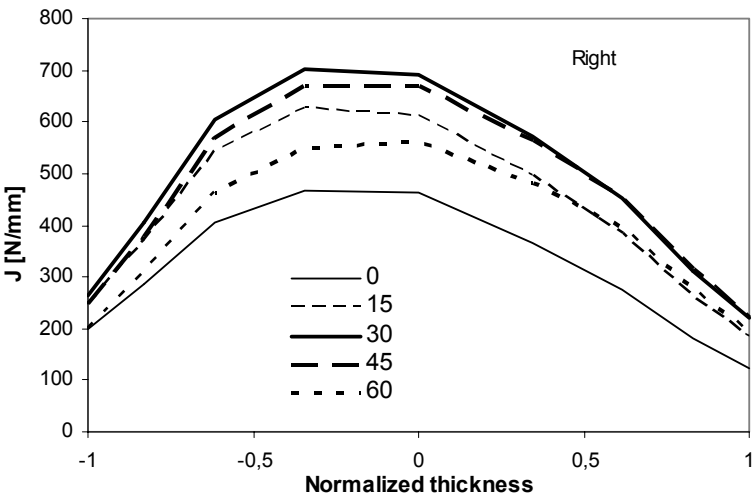

Figure 9 The J distributions along the pipe thickness for different residual stress positions for the largest crack model. (-1) indicates inside and 1 outside.

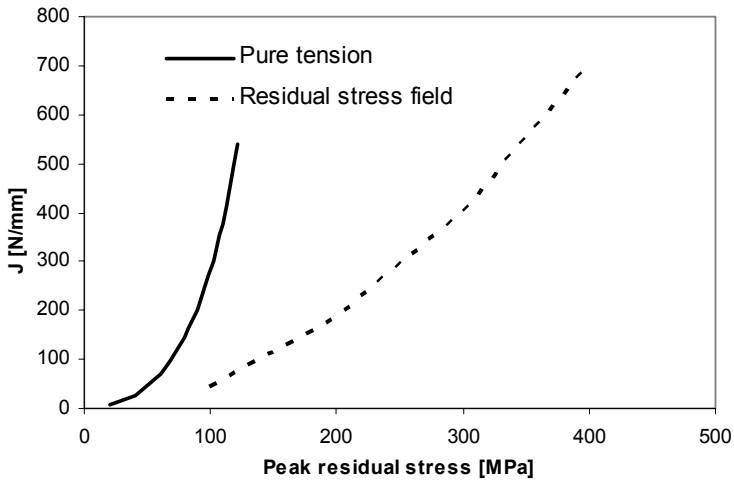

Figure 10 Comparison of the crack tip driving forces by a uniform axial residual stress and the rotated residual stress field for the crack model with the largest crack.

Fig. 10 compares the crack tip driving forces for the model with the largest crack from the failure assessment result where a uniform axial residual stress was applied at the remote end of the pipe and the highest J from a rotated residual stress field. It can be seen that the difference between the two cases are enormous. When the peak residual stress is 100 MPa, the J from a uniform residual stress is about 6 times larger than the highest J from the rotated residual stress field.

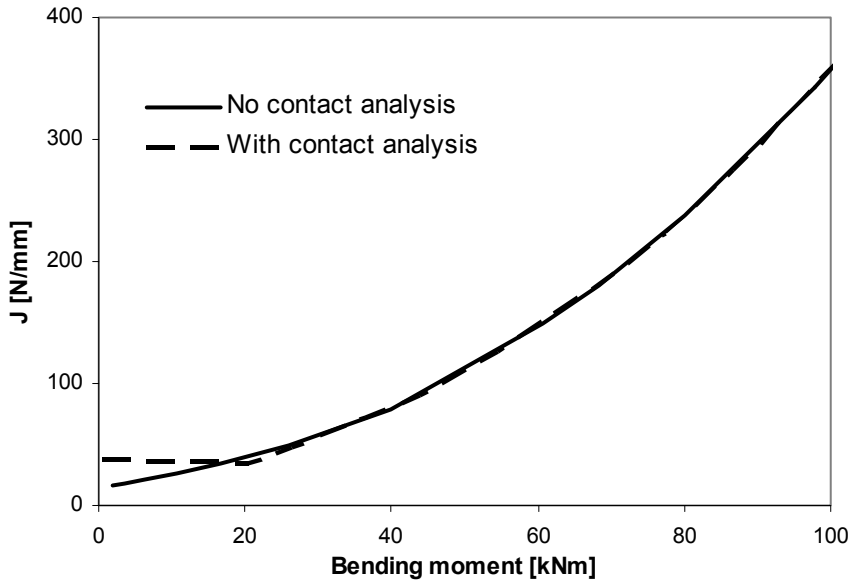

Fig. 11 The effect of surface contact on the crack tip driving forces for a case where part of the crack surfaces is located in a compressive residual stress field and part in a tensile field.

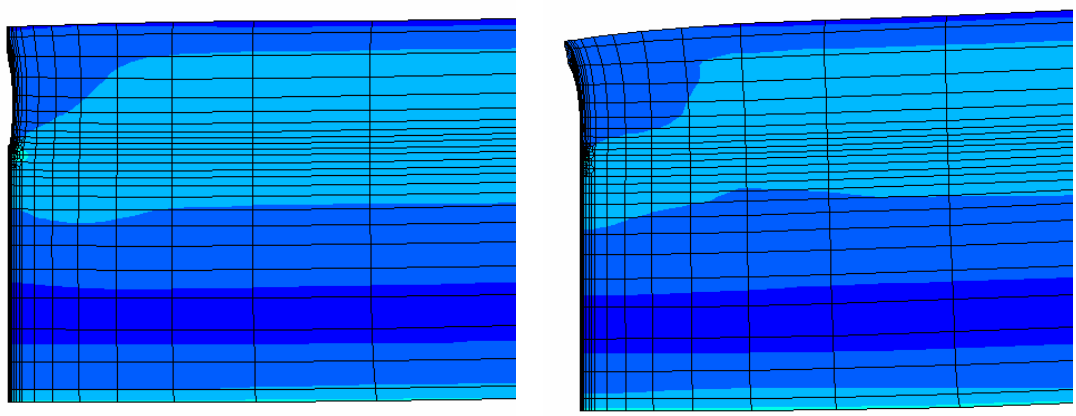

Fig. 12 Deformed meshes of the cases with and without contact elements.

When part of the cracked region is initially located in the compressive residual stress field, once the crack is introduced, the crack faces may be partly closed. If no contact elements are used in the analyses, the crack surfaces may penetrate each other. Analyses with contact elements have been performed to study the effect of this penetration on the crack tip driving force. Fig. 11 compares crack tip driving forces for the cases with and without contact elements and Fig. 12 plots the deformed meshes of these two analyses. It is interesting to observe from Fig. 11 that in the case

when the crack tip and crack front are located in tensile residual stress fields and the crack surfaces are partly located in compressive fields, the crack tip driving forces will be increased when contact elements are used in the analyses to prevent the penetration. However, when external load is high enough, analyses with and without contact elements result in no difference in the crack tip driving forces.

4. Conclusions

A parameter study on reeling-induced residual stresses has been carried out in this study. It has been shown that the final residual stress distribution is influenced by the yield strength and hardening model. However, the peak residual stresses at 8 and 10 o'clock positions are relatively stable and are in the range between 0.4 and 0.6 times of the yield stress. For high strength steels, the peak stresses at 6 and 12 o'clock positions will be generally smaller than the yield stress.

The effect of reeling-induced residual stress field has been taken into account in full pipe three dimensional analyses. The effect of residual stress on the fracture behavior is complicated. Both the crack size and the position of the residual stress field will influence the crack tip driving force. There is no analytical solution on which position gives rise to the most critical crack tip loading for a given crack size. The residual stresses have to be rotated at several angles with respect to the symmetry plane to find the critical position. The rotated position, which results in the highest J-integral due to a residual stress field, is not necessarily the critical position for the case when an external loading is applied. It has been generally observed that assessment of residual stress based on the peak value is far too conservative. This conservatism is, however, dependent on the material hardening and crack size. Further research efforts are needed to identify industrial relevant cases and establish better treatment procedure for residual stress.

References

1. F A Kandil, J D Lord, A T Fry and P V Grant, A Review of Residual Stress Measurement Methods - A Guide to Technique Selection, NPL Report MATC (A) 04, 2001.

2. J. Ødegård, C. Thaulow, K. O. Halsen and M. Bårde, Installation of Titanium pipelines by reeling – strain analyses and material properties. Proceedings of the 17th Conference on Offshore Mechanics and Artic Engineering OMAE 98, Lisbon, 6-9 July, 1998.

3. D. M. Finch and F. M. Burdekin, Effects of welding residual stresses on significance of defects in various types of welded joint, *Engineering Fracture Mechanics*, **41**, 721-735, 1992.

4. D. M. Finch, Effects of welding residual stresses on significance of defects in various types of welded joint – II, *Engineering Fracture Mechanics* **42**, 479-500, 1992.